Multi-frame blind deconvolution: Compact and multi-channel versions

Douglas A. Hope and Stuart M. Jefferies

Institute for Astronomy, University of Hawaii, 34 Ohia Ku Street, Pukalani, HI 96768, USA

ABSTRACT

We investigate two variations of the classic multi-frame blind deconvolution (MFBD) algorithm. The first is compact MFBD, a technique for reducing the number of unknown variables in the MFBD problem while still maintaining leverage from all available data frames. The second is a multi-channel MFBD algorithm. We demonstrate the performance of the former using real ground-based imagery of a satellite and show that it produces an image with fewer artifacts than were obtained with conventional MFBD. We demonstrate the performance of the latter using simulated imagery from two telescopes with different sized apertures, and show that data included from the smaller aperture telescope can facilitate an improved restoration over that obtained using solely the data from the large aperture telescope. Both variations of the MFBD technique have application in space situational awareness.

BACKGROUND

Multi-frame blind deconvolution (MFBD) is an image restoration technique developed in the early 1990s [1,2] that allows for the reconstruction of an image from multiple blurred and noisy observations, without prior knowledge on the point-spread functions (PSFs) for the observations. With this capability, it is clear why MFBD has rapidly found application in numerous areas of research including astronomy, remote sensing, medical imaging, microscopy and space situational awareness.

MFBD algorithms typically estimate the object and PSFs that describe the observed data through minimization of a cost function that has the form

$$\text{cost} = \text{data fit terms} + \text{prior terms}.$$

Here the data fit term compares the observed data with the model for the data generated from the object and PSF models. The 'prior terms' inject additional information that may be known about the imaging system or the noise processes corrupting the data. The underlying assumption is that the more prior information injected into the problem, the higher the fidelity of the solution.

In Fourier space the data fit term can be described by $\sum_{k=1}^{K}\sum_{u} M_k(u)\left|G_k(u)-\hat{G}_k(u)\right|^2$ where K is the number of data frames that are to be modeled, $G_k(u)$ is the Fourier transform of the kth data frame, $\hat{G}_k(u)$ is the model of that frame and $M_k(u)$ is a mask that is unity where the signal-to-noise ratio (SNR) is greater than one.

The prior terms come in many forms - some physical, some not (e.g., a widely-used entropy prior may be suitable for describing atoms in a box, but it is not physically meaningful for the

imaging of complex scenes). Here we introduce two (physical) priors that are based on the observation that in the case of noise-free data, the ratio of the Fourier spectra of two data frames $G_k(u)/G_{k'}(u)$ is independent of the object spectrum $F(u)$ (assuming the object is the same in each frame [3,4]). That is,

$$G_k(u)/G_{k'}(u) = \left[F(u)H_k(u) + N_k(u)\right] / \left[F(u)H_{k'}(u) + N_{k'}(u)\right] \rightarrow H_k(u)/H_{k'}(u)$$

for $N_k(u) = N_{k'}(u) = 0$ where $\hat{H}_k(u)$ is the optical transfer function, $N_k(u), N_{k'}(u)$ are the additive noise components for the k^{th} and k'^{th} frames and the PSFs are assumed to be spatially invariant and incoherent.

The first of our "spectral ratio" based prior terms enforces consistency between the estimated PSFs and is given by $\sum_{k=1}^{K}\sum_{k'>k}\sum_{u} M_{kk'}(u)\left|G_k(u)\hat{H}_{k'}(u) - G_{k'}(u)\hat{H}_k(u)\right|^2$. Here $M_{kk'}(u)$ is a mask that is unity where both $G_k(u)$ and $G_{k'}(u)$ have SNR>1.

Our second spectral ratio-based prior term enforces positivity on the estimates for the PSFs and is given by $\sum_{k=1}^{K}\sum_{j>k}^{J}\sum_{x-ve}\left|F^{-1}\left\{M_{jk}(u)\hat{H}_k(u)\frac{G_j(u)}{G_k(u)}\right\}\right|^2$ where $F^{-1}\{A\}$ denotes the inverse Fourier transform of A, $M_{j,k}(u)$ is a similar mask to $M_{kk'}(u)$ and the summation over x is only over pixels with negative values. This prior has application only in the case when the user wants to perform "compact" MFBD (CMFBD), where the object and PSFs are explicitly modeled for a subset of the data frames (K "control" frames) but all the data frames (N) are used to leverage the restoration [4]. Such a case can occur when N is very large and the number of variables required to model all the data is impractical due the large dimensionality of the parameter hyperspace. This leads to inevitable entrapment in local minima during the optimization. In CMFBD the J ($= N - K$) "non-control" frames still provide leverage on the restoration through this prior that demands that the PSFs for the non-control frames be positive. These PFSs are estimated via spectral ratios, and the PSF estimates for the control frames are modeled as a band-limited positive function. This prior provides a "hard" constraint for an object whose Fourier spectrum extends over the entire spatial frequency range sampled by the atmospheric OTFs (e.g. a star). But this is only a "soft" constraint for an object with a more compact Fourier spectrum that does not fully cover the OTF spectral extent. Here "hard" means that the constraint can be enforced throughout the optimization, while "soft" means the constraint can only be used to guide the restoration at the beginning of the optimization.

We note that both spectral ratio-based priors enforce the inherent temporal variations in the data that are due to the PSFs. Moreover, both priors can easily be extended to the case where we have additional data from more than one channel (e.g., phase diversity data or data from multiple apertures). Then, we just duplicate the cost function terms described above for the additional channels. However, it is important to note that for the multi-channel scenario there are additional "cross-channel" spectral ratios, $G_k^l(u)/G_{k'}^{l'}(u)$, that can be used to bolster the PSF consistency prior that has been introduced above. For multi-channel data the objective function becomes

$$\alpha_1 \sum_{l=1}^{L} \sum_{k=1}^{K} \sum_{u} M_k^l(u) \left| G_k^l(u) - \hat{G}_k^l(u) \right|^2 +$$

$$\alpha_2 \sum_{l=1}^{L} \sum_{l'=1}^{L} \sum_{k=1}^{K} \sum_{k'>k} \sum_{u} M_{k,k'}^{l,l'}(u) \left| G_k^l(u) \hat{H}_{k'}^{l'}(u) - G_{k'}^{l'}(u) \hat{H}_k^l(u) \right|^2 +$$

$$\alpha_3 \sum_{l=1}^{L} \sum_{k=1}^{K} \sum_{j>k}^{J} \sum_{x-ve} \left| F^{-1} \left\{ M_{j,k}^l(u) \hat{H}_k^l(u) \frac{G_j^l(u)}{G_k^l(u)} \right\} \right|^2$$

where α_i are weights that are adjusted so that the derivatives of the cost function with respect to each variable are balanced across the terms [4] and L is the number of data channels.

This general cost function is applicable to both MFBD ($J = 0$) and CMFBD ($J \neq 0$). Please note that it is easy to show that for $L = 1$, $J \neq 0$ and $\alpha_2 = 0$, this cost function is identical to that obtained with Equations (5) and (10) in [4]. In addition, for $\alpha_2 = \alpha_3 = 0$, this cost function reduces to that used in what we refer as "traditional" MFBD, where positivity on the object and PSFs is enforced as part of their physical model.

In this paper, we study two implementations of this general cost function: $J \neq 0, L = 1, \alpha_2 > 0, \alpha_3 > 0$ and $J = 0, L = 2, \alpha_2 = \alpha_3 = 0$. The former represents single channel CMFBD, the latter multi-channel MFBD.

COMPACT MFBD

We evaluate the performance of our CMFBD algorithm using real ground-based imagery of the SEASAT remote sensing satellite observed in the near infrared using the GEMINI 1.6m telescope on Haleakala (Maui) during daytime. We use $N = 271$ data frames with $K = 36$ control frames. Examples of the data frames are shown in the upper two panels of Fig 1. Please refer to [4] for details of the modeling of the object and the PSFs, and the general implementation of CMFBD. On the lower left is a restoration using a conventional MFBD algorithm [5], while the lower right is the CMFBD restoration which was obtained by setting $\alpha_1 = 1, \alpha_2 = \alpha_3 = 0.1$ with the soft positivity constraint metric (the second spectral ratio-based prior term) held until the change in its value was less than 10% which occurred after about 80 iterations for this particular target. The consistency metric was enforced for the entire minimization. The main bar across the image represents the down-looking synthetic aperture radar antenna, and the two panels extending out represent the solar panels. On comparing the two images, it is clearly noticeable that the solar panels are more well-defined and there is an obvious decrease in the number of artifacts in the CMFBD image.

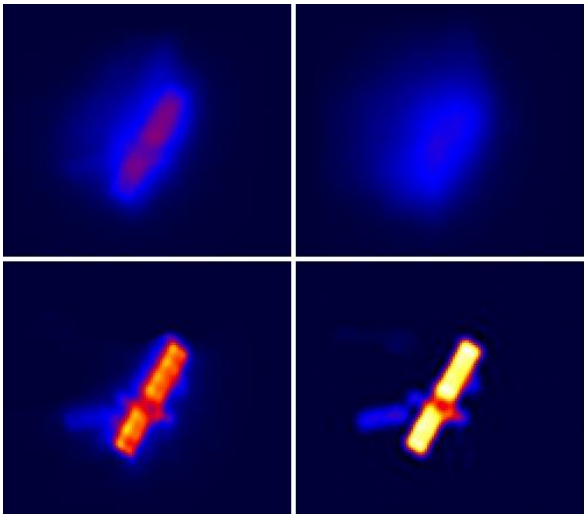

Figure 1 Top left: best data frame. Top Right: worst data frame. Bottom Left: Restoration using a conventional MFBD algorithm [5]. Bottom right: Restoration using the CMFBD algorithm

MULTI-CHANNEL MFBD

Here, we study the possibility of using multi-channel MFBD with focal plane imagery obtained from two telescopes $(L = 2, J = 0, \alpha_2 = \alpha_3 = 0)$ to improve the fidelity of the restored image of the object over what can be obtained from a single telescope. The telescopes have different apertures and are in proximity to each other, such that the target object presents the same pose to each telescope.

For our preliminary tests we use simulations of imagery obtained simultaneously with 3.6m and 1.6m telescopes. We assume an object of visual magnitude 2.3 and turbulence conditions characterized by $D/r_0 = 27$ for the 3.6m telescope. Please note that adaptive optics is not effective in these conditions. The image cadence for both telescope systems is 50 frames per second and both cameras have the same field scale. The image data are noise free, as we want to investigate the ability of our restoration algorithm to unscramble the turbulence problem.

To study the effect of adding a second data channel, we ran MFBD for two scenarios - both with the same total photon count (6×10^7 photons). This is to ensure that same amount of information is available in each scenario. The first test used 6 frames of 3.6 m data, and the second used 4 frames of 3.6 m data and 10 frames of 1.6 m data. Due to the aperture sizes, the number of photons collected in 10 data frames from the 1.6 meter is equivalent to the total photons in two data frames from the 3.6m telescope.

The restorations were run for 5000 iterations. The results, shown in Fig. 2, clearly show that there is a marked improvement in image fidelity when using the data from both telescopes. We infer that this gain comes through better constraining of the low spatial frequencies during the restoration process. Fig. 3 shows that this result is robust even in the presence of noise on the data.

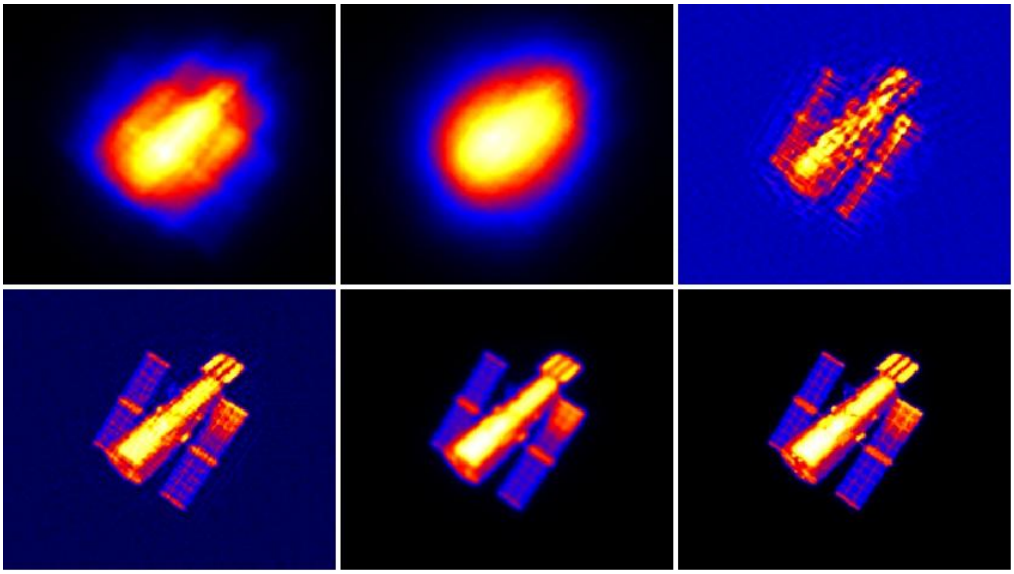

Figure 2 Top Row: Data frame from GEMINI 1.6m on left, data frame from AEOS 3.6m in center. On the right is a restoration of the AEOS imagery (6 frames). Bottom Row: MFBD restoration of both AEOS imagery (4 frames) and GEMINI imagery (10 frames) on the left. The diffraction-limited image for the GEMINI 1.6m is shown in the center and the diffraction-limited image for the AEOS 3.6m on the right. Observations are at 0.90 microns.

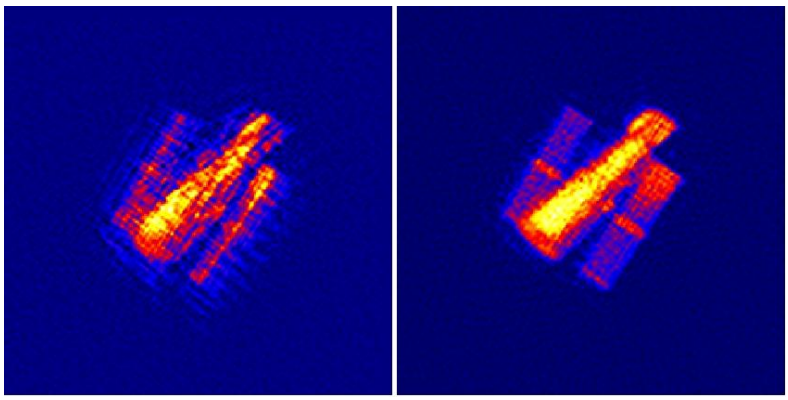

Figure 3 Shown are restorations in the presence of photon counting noise. Left: restoration using 6 noise corrupted data frames from the 3.6m telescope and Right: Restoration of imagery using both 3.6m data (4 frames) and 1.6m data (10 frames) .

DISCUSSION

MFBD is a difficult mathematical and computational problem that has received significant attention in recent years due to its wide applicability. The mantra of MFBD practitioners has been "the more physical constraints used, the better the restoration". Indeed, our preliminary results shown above for the compact and multi-frame variations of MFBD support this philosophy. In particular, we have validated CMFBD using real data and have shown that there is a potentially significant benefit to fusing data from telescopes with different sized apertures. Having said that, we note that while our results for the multi-channel approach are

extremely encouraging, further studies need to be performed to understand the range of conditions where such an approach will be effective.

As more and more data channels are used to provide additional constraints on the MFBD problem, the number of variables required to model all the data unfortunately exceeds practical levels. This happens both computationally due to memory limitations and mathematically, when the dimensionality of the parameter hyperspace becomes extremely large, leading to inevitable entrapment in local minima during the optimization. Our results indicate that the merging of the compact and multi-channel extensions of MFBD offers a way to overcome this limitation. Additionally, it also provides a possibility for an extension of MFBD research to potential scenarios consisting of datasets that are orders of magnitude larger than those currently processed.

ACKNOWLEDGEMENTS

This study was supported by award F9550-09-1-0216 from the Air Force Office of Scientific Research. Simulations were run using computing resources at the Maui High Performance Computing Center.

REFERENCES

[1] T. J. Schulz, "Multi-frame blind deconvolution of astronomical images", *JOSA A.*, 10, 1064-1073 (1993)

[2] S. M. Jefferies and J. Christou, "Restoration of Astronomical Images by Iterative Blind Deconvolution", *Ap.J.*, 415, 862-864 (1993)

[3] B. R. Frieden, "An exact, linear solution to the problem of imaging through turbulence", *Optics Communications*, 150, 15-21 (1998)

[4] D. A. Hope and S. M. Jefferies, "Compact multi-frame blind deconvolution", *Optics Letters*, 36, 867-869 (2011).

[5] Charles L. Matson, Kathy Borelli, Stuart Jefferies, Charles C. Beckner, Jr., E. Keith Hege, and Michael Lloyd-Hart, "Fast and optimal multiframe blind deconvolution algorithm for high-resolution ground-based imaging of space objects," Appl. Opt. 48, A75-A92 (2009)